

Journal of
Mechanics of
Materials and Structures

FREE FLEXURAL VIBRATIONS OF MASONRY BEAM-COLUMNS

Maria Girardi and Massimiliano Lucchesi

Volume 5, N° 1

January 2010

 mathematical sciences publishers

FREE FLEXURAL VIBRATIONS OF MASONRY BEAM-COLUMNS

MARIA GIRARDI AND MASSIMILIANO LUCCHESI

We present an analytical study of the free transverse vibrations of masonry beam-columns, focusing on the role of the material's inability to sustain traction in modifying the dynamic behavior of such structures. In particular, for periodic oscillations, an analytical method is presented for obtaining an explicit relation between the fundamental frequency of the beam and the displacement amplitude.

1. Introduction

In recent years, the dynamic response of age-old masonry structures and buildings has attracted growing interest, particularly in Italy, where the extraordinary historical architectural heritage is regularly threatened by violent earthquakes. Much effort has been devoted to evaluating the seismic vulnerability of such structures. The methods developed are based mainly on a classification of the damage mechanisms consequent to earthquakes [Petrini et al. 1999; MiBAC 2006] and application of some simplification procedures, which have been adopted by Italian regulations [Norme tecniche 2008]. A number of mechanical models have been developed and implemented in numerical codes, involving a limited number of degrees of freedom and developed for the most part by defining macro-elements [Petrini et al. 1999; Gambarotta and Lagomarsino 1997].

The dynamic behavior of masonry structures is heavily influenced by a variety of parameters, such as construction technique, construction geometry, material characteristics, and type of accelerations applied to the structural supports. Moreover, masonry structures respond differently to tensile and compressive stresses.

In the 1980s [Del Piero 1989; Di Pasquale 1992], a constitutive equation was formulated to describe the behavior of a class of materials, termed no-tension or masonry-like, that is able to withstand compressive stresses but only limited or null tensile stresses. This approach appeared to provide a satisfactory description of the main aspects of the static behavior of old masonry buildings [De Falco and Lucchesi 2002; Lucchesi et al. 2008].

A numerical model was proposed in [Lucchesi and Pintucchi 2007] to describe the dynamic behavior of slender masonry structures, such as columns or towers, by means of one-dimensional finite elements. This model is based on a no-tension constitutive equation expressed in terms of generalized stresses and strains [Zani 2004]. The nonlinear elastic material described by the model provides satisfactory

Keywords: no-tension materials, masonry slender structures, nonlinear dynamics.

The financial supports of the Italian Ministry of University and Research (Project "Diagnostica e salvaguardia di manufatti architettonici con particolare riferimento agli effetti derivanti da eventi sismici e altre calamità naturali") and of the Region of Tuscany (Project "Sciences and Technologies for the Tuscany Artistic, Architectural and Archeological Heritage" – ST@RT) are gratefully acknowledged.

predictions for the dynamic behavior of such structures. The model mainly predicts flexural oscillations and does not include material damage under cyclic stresses.

In this paper, we present a study of the flexural dynamic behavior of slender masonry structures with the aim of finding an explicit relation between a beam's fundamental frequency and the total energy of the system. We begin with the constitutive law described in [Zani 2004] and used in [Lucchesi and Pintucchi 2007].

The spread of cracks along a beam reduces the stiffness of a structure and gives rise to interactions between the natural beam oscillation frequencies and the amplitude of the cracked zone. These effects strongly alter the dynamic behavior of slender masonry structures, which are characterized by a response to acceleration that deviates considerably from linearity.

Relations between frequencies and amplitudes have been found for several types of softening systems [Nayfeh and Mook 1995; Nayfeh 2000] mainly by using perturbation methods, such as the multiple scales method or averaging techniques. However, such relations may be obtained directly from the equations of motion, as shown in [Whitham 1974] for the propagation of waves in dispersive media.

This work is divided into three parts. Section 2 presents an equation describing the dynamic equilibrium of a one-dimensional continuous beam composed of an elastic material. Then, under suitable hypotheses regarding the form of the solution, a relation between the fundamental frequency and the energy of the system is deduced.

In the two subsequent sections, comprising the second part of the paper, we apply this relation to a masonry beam. Section 3 is dedicated to materials described by the no-tension constitutive equation, and Section 4 introduces a simplified cubic polynomial constitutive law that can approximate the no-tension relation for curvature values near the elastic limit.

Lastly, Section 5 presents some example applications and makes a comparison between the analytical results and the corresponding numerical solutions obtained via the code described in [Lucchesi and Pintucchi 2007].

All results presented here were obtained assuming conservative systems and free vibrations. Future work will study forced and damped oscillations; some results of this kind can already be found in [Girardi 2009; Girardi and Lucchesi 2006].

2. Formulation of the dynamic problem

Consider a rectilinear beam with length l and rectangular cross-section characterized by height h and width b , subjected to a uniform axial force N . Let χ be the curvature of the beam and $M(\chi) : R \rightarrow R$ be the bending moment, a continuous differentiable function with a second derivative that is assumed to be piecewise continuous. Let E and ρ denote the Young modulus and density of the material, respectively, and $J = bh^3/12$ denotes the moment of inertia of the beam's cross-section.

To work with dimensionless quantities, if x and v are, respectively, the abscissa along the beam's axis and the transverse flexural displacement of the beam (see Figure 1), and t denotes time, we define

$$\xi = \frac{x}{l}, \quad \tau = \frac{t}{T_c}, \quad u = \frac{v}{l}, \quad \kappa = \chi l, \quad (2-1)$$

where $T_c = l^2/c$ and $c = \sqrt{\frac{EJ}{\rho bh}}$ are the elastic constants of the beam.

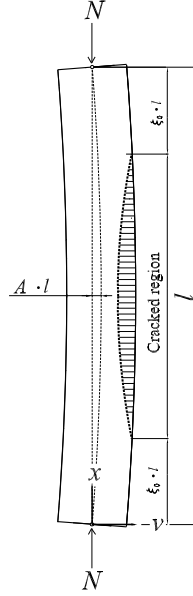


Figure 1. A masonry beam-column: model and notations.

We assume the effects of both the shear strain and the rotary inertia to be negligible. Moreover, we limit ourselves to considering situations in which the flexural displacement $u(\zeta, \tau)$ and its derivative $u_\zeta(\zeta, \tau)$ are small, so that we can neglect the effects of the axial force on the dynamic equilibrium of the beam, and write

$$\kappa(\zeta, \tau) = -u_{\zeta\zeta}(\zeta, \tau). \tag{2-2}$$

Under these hypotheses, set

$$f(\kappa) = \frac{l}{EJ} M(\kappa/l), \tag{2-3}$$

the equation of motion is

$$\frac{\partial^2 u}{\partial \tau^2} - \frac{\partial^2 (f \circ \kappa)}{\partial \zeta^2} = 0, \tag{2-4}$$

which coincides with the Euler equation

$$\frac{\partial}{\partial \tau} \left(\frac{\partial L}{\partial u_\tau} \right) - \frac{\partial^2}{\partial \zeta^2} \left(\frac{\partial L}{\partial u_{\zeta\zeta}} \right) = 0, \tag{2-5}$$

corresponding to the Lagrangian

$$L = \frac{1}{2} (u_\tau)^2 - F(-u_{\zeta\zeta}), \tag{2-6}$$

where F is the primitive of f such that $F(0) = 0$, as can be easily verified. The goal is to find approximate solutions to (2-4) of the form [Nayfeh and Mook 1995; Nayfeh 2000]

$$u(\zeta, \tau) = \sum_{i=1}^n \phi_i(\zeta) \eta_i(\tau), \tag{2-7}$$

where the functions ϕ_i are twice continuously differentiable and satisfy the orthogonality condition

$$\int_0^1 \phi_i \phi_j = \delta_{ij} \quad \text{for } i, j \in 1 \dots n. \quad (2-8)$$

From (2-6), we deduce that

$$L = L(\phi_i, \phi_i'', \eta_i, \eta_i') = \frac{1}{2} \left(\sum_{i=1}^n \phi_i \eta_i' \right)^2 - F \left(- \sum_{i=1}^n \phi_i'' \eta_i \right), \quad (2-9)$$

where the primes denote differentiation.

Let us introduce the averaged Lagrangian \bar{L} over the normalized length of the beam

$$\bar{L}(\eta_i, \eta_i') = \int_0^1 L(\phi_i, \phi_i'', \eta_i, \eta_i') d\xi = \frac{1}{2} \int_0^1 \left(\sum_{i=1}^n \phi_i \eta_i' \right)^2 d\xi - \int_0^1 F \left(- \sum_{i=1}^n \phi_i'' \eta_i \right) d\xi. \quad (2-10)$$

By virtue of (2-8), we can write

$$\bar{L}(\eta, \eta') = \frac{1}{2} \sum_{i=1}^n \eta_i'^2 - V(\eta_i), \quad (2-11)$$

where

$$V(\eta_i) = \int_0^1 F \left(- \sum_{i=1}^n \phi_i'' \eta_i \right) d\xi. \quad (2-12)$$

First, we will verify that each function η_i satisfies the equation

$$\frac{\partial}{\partial \tau} \frac{\partial \bar{L}}{\partial \eta_i'} - \frac{\partial \bar{L}}{\partial \eta_i} = 0. \quad (2-13)$$

To this aim, we observe that

$$\frac{\partial L}{\partial u_\tau} = \sum_{j=1}^n \frac{1}{\phi_j} \frac{\partial L}{\partial \eta_j'}, \quad \frac{\partial L}{\partial u_{\xi\xi}} = \frac{1}{n} \sum_{j=1}^n \frac{1}{\eta_j} \frac{\partial L}{\partial \phi_j''}, \quad (2-14)$$

and, thus, from (2-5), we obtain

$$\sum_{j=1}^n \frac{1}{\phi_j} \frac{\partial}{\partial \tau} \left(\frac{\partial L}{\partial \eta_j'} \right) - \frac{1}{n} \sum_{j=1}^n \frac{1}{\eta_j} \frac{\partial^2}{\partial \xi^2} \left(\frac{\partial L}{\partial \phi_j''} \right) = 0. \quad (2-15)$$

Now, multiplying (2-15) by each ϕ_i and integrating over $[0, 1]$, we obtain the set of equations

$$\frac{\partial}{\partial \tau} \left(\frac{\partial \bar{L}}{\partial \eta_i'} \right) + \sum_{j \neq i} \int_0^1 \frac{\phi_i}{\phi_j} \frac{\partial}{\partial \tau} \frac{\partial L}{\partial \eta_j'} - \frac{1}{n} \int_0^1 \phi_i \sum_{j=1}^n \frac{1}{\eta_j} \frac{\partial^2}{\partial \xi^2} \frac{\partial L}{\partial \phi_j''} d\xi = 0. \quad (2-16)$$

In view of (2-9) and (2-8), equation (2-16) becomes

$$\frac{\partial}{\partial \tau} \left(\frac{\partial \bar{L}}{\partial \eta_i'} \right) + \sum_{j \neq i} \int_0^1 \frac{\phi_i}{\phi_j} \frac{\partial}{\partial \tau} (\phi_j^2 \eta_j') - \frac{1}{n} \int_0^1 \phi_i \sum_{j=1}^n \frac{1}{\eta_j} \frac{\partial^2 f}{\partial \xi^2} \eta_j d\xi = \frac{\partial}{\partial \tau} \frac{\partial \bar{L}}{\partial \eta_i'} - \int_0^1 \frac{\partial^2 f}{\partial \xi^2} \phi_i d\xi = 0, \quad (2-17)$$

where, for the sake of brevity, we write $\partial^2 f / \partial \xi^2$ for $\partial^2 (f \circ \kappa) / \partial \xi^2$.

Now, under the assumption that $f' \phi_i = \phi_i' f = 0$ at the ends of the beam, we obtain

$$\begin{aligned} \frac{\partial}{\partial \tau} \frac{\partial \bar{L}}{\partial \eta_i'} - \int_0^1 \frac{\partial^2 f}{\partial \xi^2} \phi_i d\xi &= \frac{\partial}{\partial \tau} \frac{\partial \bar{L}}{\partial \eta_i'} - \frac{\partial f}{\partial \xi} \phi_i \Big|_0^1 + \int_0^1 \frac{\partial f}{\partial \xi} \phi_i' d\xi \\ &= \frac{\partial}{\partial \tau} \frac{\partial \bar{L}}{\partial \eta_i'} + f \phi_i' \Big|_0^1 - \int_0^1 f \phi_i'' d\xi = \frac{\partial}{\partial \tau} \frac{\partial \bar{L}}{\partial \eta_i'} - \int_0^1 f \phi_i'' d\xi. \end{aligned} \quad (2-18)$$

From (2-10), we deduce that

$$\frac{\partial \bar{L}}{\partial \eta_i} = -\frac{\partial}{\partial \eta_i} \int_0^1 F\left(-\sum_{j=1}^n \phi_j'' \eta_j\right) d\xi = \int_0^1 f \phi_i'' d\xi, \quad (2-19)$$

and (2-13) follows from (2-18).

Because $f(\kappa)$ is, in general, a nonlinear function, the corresponding equations (2-13) are coupled. For our purposes, it is sufficient to limit ourselves to unimodal solutions of the form

$$u(\xi, \tau) = \phi(\xi)\eta(\tau), \quad (2-20)$$

and, thus, (2-13) reduces to

$$\frac{\partial}{\partial \tau} \frac{\partial \bar{L}}{\partial \eta'} - \frac{\partial \bar{L}}{\partial \eta} = 0. \quad (2-21)$$

If we set

$$\eta = \eta(\theta), \quad \theta_\tau = \omega, \quad (2-22)$$

where the frequency ω indicates a slowly varying system parameter [Whitham 1974], and

$$\bar{L}_1 = \frac{\partial \bar{L}}{\partial \eta'}, \quad \bar{L}_2 = \frac{\partial \bar{L}}{\partial \eta}, \quad (2-23)$$

then equation (2-21) becomes $\omega \frac{\partial \bar{L}_1}{\partial \theta} - \bar{L}_2 = 0$. Multiplying this by $\frac{\partial \eta}{\partial \theta}$, and recalling that

$$\frac{\partial \bar{L}}{\partial \theta} = \omega \frac{\partial^2 \eta}{\partial \theta^2} \bar{L}_1 + \bar{L}_2 \frac{\partial \eta}{\partial \theta}, \quad (2-24)$$

we obtain

$$\omega \frac{\partial \bar{L}_1}{\partial \theta} \frac{\partial \eta}{\partial \theta} - \frac{\partial \bar{L}}{\partial \theta} + \bar{L}_1 \omega \frac{\partial^2 \eta}{\partial \theta^2} = \frac{\partial}{\partial \theta} \left(\omega \bar{L}_1 \frac{\partial \eta}{\partial \theta} \right) - \frac{\partial \bar{L}}{\partial \theta} = 0, \quad (2-25)$$

whose first integral is

$$\omega \bar{L}_1 \frac{\partial \eta}{\partial \theta} - \bar{L} = a, \quad (2-26)$$

where a is the total energy of the system, which is constant with respect to θ and is related to the amplitude of the motion.

In view of (2-11), with $i = 1$, equation (2-26) becomes

$$\frac{1}{2} \omega^2 \left(\frac{\partial \eta}{\partial \theta} \right)^2 + V(\eta) = a, \quad (2-27)$$

from which we have $\frac{d\theta}{d\eta} = \frac{\omega}{\sqrt{2(a - V(\eta))}}$. Then,

$$\frac{2\pi}{\omega} = \oint \frac{d\eta}{\sqrt{2(a - V(\eta))}}, \tag{2-28}$$

where the integral is taken over a complete loop of the motion [Whitham 1974].

Equation (2-28) links the frequency ω to the total energy a of the system and is exactly the relation we are seeking.

3. No-tension material

3A. The constitutive equation. Let the beam described in Section 2 be composed of a no-tension material with zero tensile strength and infinite compressive strength (see Figure 2).

Let ε denote an infinitesimal axial deformation. Under the classical Euler–Bernoulli hypothesis, we can deduce a relation between the generalized deformations ε and χ and the generalized stresses N and M . For each normal section of the beam, let

$$\Sigma = \{(N, M) : N \leq 0, \frac{1}{2}Nh \leq M \leq -\frac{1}{2}Nh\} \tag{3-1}$$

be the set of all admissible generalized stresses, and let us consider the subsets of Σ (see Figure 2)

$$\begin{aligned} \Sigma_1 &= \{(N, M) \in \Sigma : \frac{1}{6}Nh \leq M \leq -\frac{1}{6}Nh\}, \\ \Sigma_2 &= \{(N, M) \in \Sigma : -\frac{1}{6}Nh \leq M \leq -\frac{1}{2}Nh\}, \\ \Sigma_3 &= \{(N, M) \in \Sigma : \frac{1}{2}Nh \leq M \leq \frac{1}{6}Nh\}. \end{aligned} \tag{3-2}$$

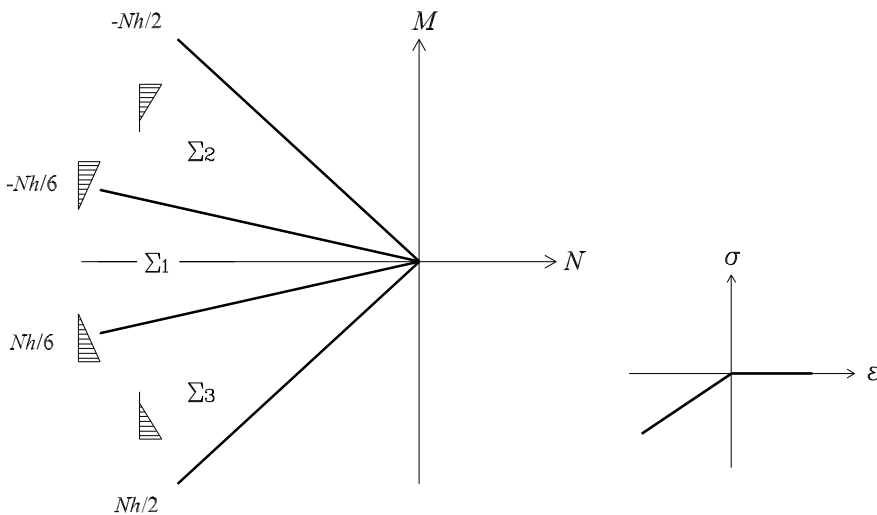


Figure 2. The σ - ε relation for a no-tension material with infinite compressive strength and zero tensile strength and the admissible generalized stresses M, N for a rectangular section of height h .

Then, we can write the constitutive equation [Zani 2004]:

$$\begin{aligned}
 (N, M) \in \Sigma_1: \quad \varepsilon &= \frac{N}{Ebh}, & \chi &= \frac{12M}{Ebh^3}, \\
 (N, M) \in \Sigma_2: \quad \varepsilon &= \frac{8}{9Eb} \frac{N^2(Nh+3M)}{(Nh+2M)^2}, & \chi &= -\frac{8}{9Eb} \frac{N^3}{(Nh+2M)^2}, \\
 (N, M) \in \Sigma_3: \quad \varepsilon &= \frac{8}{9Eb} \frac{N^2(Nh-3M)}{(Nh-2M)^2}, & \chi &= -\frac{8}{9Eb} \frac{N^3}{(Nh-2M)^2}.
 \end{aligned} \tag{3-3}$$

(N, M) in Σ_1 corresponds to a fully compressed section. Σ_2 and Σ_3 correspond to regions in which the section is only partially compressed. The outer boundaries of Σ_2 and Σ_3 are reached when the eccentricity M/N in the section is equal to $-h/2$ and $h/2$, respectively, corresponding to a situation that is allowed given that the material is assumed to have infinite compressive strength.

Equations (3-3) can be inverted to obtain $N = N(\varepsilon, \chi)$, $M = M(\varepsilon, \chi)$. To this aim, we introduce the subsets of the set E of all generalized strains (ε, χ) :

$$\begin{aligned}
 E_1: \quad & \{(\varepsilon, \chi) \in E : 2\varepsilon \leq \chi h \leq -2\varepsilon, \varepsilon \leq 0\}, \\
 E_2: \quad & \{(\varepsilon, \chi) \in E : \chi h > 2|\varepsilon|, \chi > 0\}, \\
 E_3: \quad & \{(\varepsilon, \chi) \in E : \chi h < 2|\varepsilon|, \chi < 0\}.
 \end{aligned} \tag{3-4}$$

Then, from (3-3) we obtain

$$\begin{aligned}
 (\varepsilon, \chi) \in E_1: \quad N &= Ebh\varepsilon, & M &= \frac{Ebh^3}{12}\chi, \\
 (\varepsilon, \chi) \in E_2: \quad N &= -\frac{Eb(\chi h - 2\varepsilon)^2}{8\chi}, & M &= \frac{Eb(\varepsilon + \chi h)(\chi h - 2\varepsilon)^2}{24\chi^2}, \\
 (\varepsilon, \chi) \in E_3: \quad N &= \frac{Eb(\chi h + 2\varepsilon)^2}{8\chi}, & M &= -\frac{Eb(\varepsilon - \chi h)(\chi h + 2\varepsilon)^2}{24\chi^2}.
 \end{aligned} \tag{3-5}$$

If the axial force N acting on the section is a known quantity, then from (3-5) we can obtain a relation $M = M(\chi, N)$ between the bending moment and the curvature. To this aim, we define

$$\chi_0 = -\frac{2N}{Ebh^2}, \tag{3-6}$$

the curvature corresponding to the elastic limit. Therefore, from (3-5), we have

$$\frac{M(\chi)}{\rho bh} = \begin{cases} c^2\chi & \text{for } |\chi| \leq \chi_0, \\ c^2\chi_0 \operatorname{sign}(\chi)(3 - 2\sqrt{\chi_0/|\chi|}) & \text{for } |\chi| > \chi_0, \end{cases} \tag{3-7}$$

which represents the constitutive equation we are looking for.

The function (3-7) is plotted in Figure 3. For increasing values of χ in the nonlinear region, we see that the stiffness of the section decreases quickly and the bending moment tends toward its limit value $|Nh/2|$. Moreover, we observe that $M(\chi)$ is continuous with its first derivative, whereas the second derivative undergoes a jump in value for $|\chi| = \chi_0$.

where we have used the elliptic integral

$$E\left(\frac{\pi}{4}(1-2\xi_0), 2\right) = \int_0^{\frac{\pi}{4}(1-2\xi_0)} \frac{1}{\sqrt{1-2\sin^2\zeta}} d\zeta. \quad (3-12)$$

We can find the abscissa ξ_0 from the relation

$$|\kappa(\xi_0, \tau)| = \kappa_0, \quad (3-13)$$

such that with the help of (2-2) and (3-9), we obtain

$$\xi_0(\eta) = \frac{1}{\pi} \arcsin \frac{\kappa_0}{\pi^2 \sqrt{2} |\eta|} \quad \text{for } |\eta| \geq \frac{\kappa_0}{\pi^2 \sqrt{2}}. \quad (3-14)$$

Moreover, when the beam is entirely in the elastic field, we have

$$\xi_0(\eta) = \frac{1}{2} \quad \text{for } |\eta| < \frac{\kappa_0}{\pi^2 \sqrt{2}}. \quad (3-15)$$

Now, in view of (2-11), the potential function $V(\eta)$ for $|\eta| < \frac{\kappa_0}{\pi^2 \sqrt{2}}$ becomes

$$V_{el}(\eta) = \frac{\pi^4 \eta^2}{2}, \quad (3-16)$$

and the potential function for $|\eta| \geq \frac{\kappa_0}{\pi^2 \sqrt{2}}$ becomes

$$V_{nl}(\eta) = \pi^4 \eta^2(\tau) \xi_0 - \frac{1}{2} \pi^3 \eta^2(\tau) \sin(2\pi \xi_0) + 6\sqrt{2} \pi \kappa_0 |\eta(\tau)| \cos(\pi \xi_0) - \frac{16}{\pi} \sqrt{2\kappa_0^3 \pi^2 |\eta(\tau)|} E\left(\frac{\pi}{4}(1-2\xi_0), 2\right) - 3\kappa_0^2 \xi_0 + \frac{3}{2} \kappa_0^2. \quad (3-17)$$

In Figure 4, V is plotted as a function of η for different values of κ_0 and compared with the linear elastic case, represented by a parabolic curve.

We can now apply equations (3-16) and (3-17) to relation (2-28) and write

$$\begin{aligned} \omega &= \frac{\pi}{2} / \int_0^{R_1} \frac{d\eta}{\sqrt{2(a - V_{el}(\eta))}} = \pi^2 \quad \text{for } \eta \leq \frac{\kappa_0}{\pi^2 \sqrt{2}}, \\ \omega &= \frac{\pi}{2} / \left(\int_0^{\frac{\kappa_0}{\pi^2 \sqrt{2}}} \frac{d\eta}{\sqrt{2(a - V_{el}(\eta))}} + \int_{\frac{\kappa_0}{\pi^2 \sqrt{2}}}^{R_2} \frac{d\eta}{\sqrt{2(a - V_{nl}(\eta))}} \right) \quad \text{for } \eta > \frac{\kappa_0}{\pi^2 \sqrt{2}}, \end{aligned} \quad (3-18)$$

where R_1, R_2 are roots of the equation

$$a - V(\eta) = 0. \quad (3-19)$$

Equations (3-18) can be solved numerically for different values of the total energy a and the elastic bending limit κ_0 to obtain the curves shown in Figure 5.

By way of example, let us now consider a hinged-hinged beam subjected to an initial deformed shape

$$u(\xi, 0) = A \sin(\pi \xi), \quad A > 0. \quad (3-20)$$

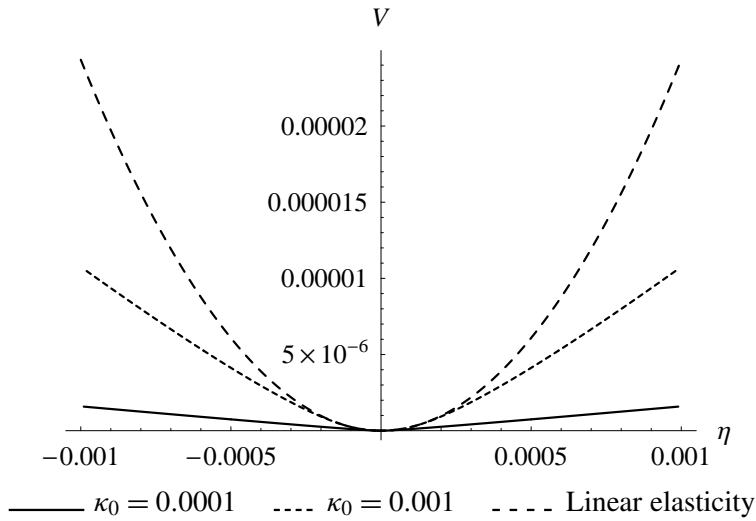


Figure 4. The potential function $V(\eta)$ for different values of κ_0 .

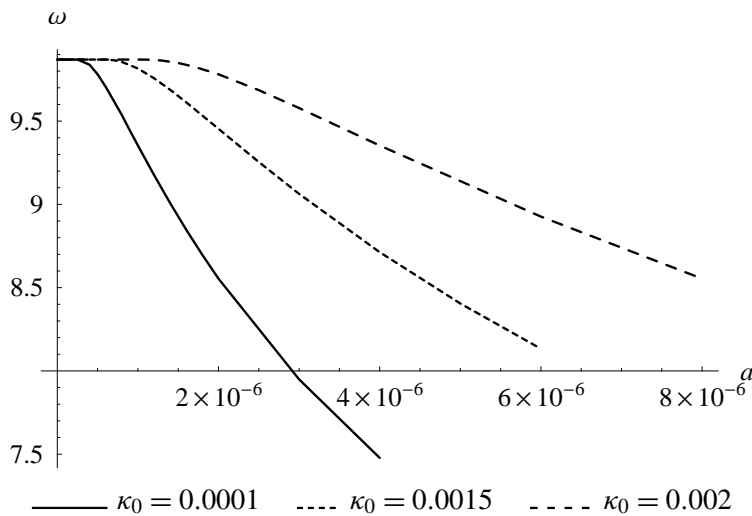


Figure 5. The function ω as a function of a , as given by (3-18), for different values of the limit-elastic curvature κ_0 .

The deformed shape of the beam is represented in Figure 1 on page 145, where $l\zeta_0$ and $l(1 - \zeta_0)$ delimit the cracked region.

The particular form chosen for the initial deformed shape, together with the absence of internal resonances in the first mode [Nayfeh and Mook 1995; Nayfeh 2000], allows us to describe the motion of the beam using the unimodal expression (3-9).

We can write the total energy a of the beam as a function of the amplitude A of the motion, observing that

$$\eta(0) = A/\sqrt{2}, \quad \eta'(0) = 0. \tag{3-21}$$

Therefore, from (3-16), we have

$$a(A, \kappa_0) = V(0) = \frac{1}{2}\pi^4 A^2 \bar{\xi}_0 - \frac{1}{4}\pi^3 A^2 \sin(2\pi \bar{\xi}_0) + 6\pi \kappa_0 A \cos(\pi \bar{\xi}_0) - \frac{16}{\pi} \sqrt{\kappa_0^3 A \pi^2} E\left(\frac{\pi}{4}(1 - 2\bar{\xi}_0), 2\right) - 3\kappa_0^2 \bar{\xi}_0 + \frac{3}{2}\kappa_0^2, \quad (3-22)$$

the initial cracked region being delimited by $1 - 2\bar{\xi}_0$ and

$$\bar{\xi}_0(A, \kappa_0) = \frac{1}{\pi} \arcsin \frac{\kappa_0}{\pi^2 A}. \quad (3-23)$$

Now, from (3-18) we can find the frequency ω of the oscillations as a function of A and κ_0 .

4. The cubic approximation

Next, we present a simpler constitutive law that approximates equation (3-7) for values of χ near χ_0 . To this aim, we introduce the cubic equation

$$\frac{M_c(\chi)}{\rho b h} = c^2 \chi (1 - \bar{\sigma} \chi^2), \quad (4-1)$$

where $\bar{\sigma}$ is a positive parameter that depends on the axial force N , which can approximate (3-7) for values of χ in the range $-\sqrt{1/3\bar{\sigma}} \leq \chi \leq \sqrt{1/3\bar{\sigma}}$, where the cubic function is increasing. Figure 6 shows a comparison of the behavior of equations (3-7) and (4-1) for a given value of N .

From (4-1), we obtain the dimensionless equation

$$F_c(\kappa) = \frac{1}{2}\kappa^2 - \sigma \frac{1}{4}\kappa^4, \quad (4-2)$$

where $\sigma = \bar{\sigma}/l^2$. This represents a classical cubic nonlinearity problem for softening systems.

If the displacement $u(\zeta, \tau)$ is again expressed by (3-9), we can write the potential

$$V(\eta) = \frac{1}{2}\pi^4 \eta^2 - \frac{3}{8}\sigma \pi^8 \eta^4. \quad (4-3)$$

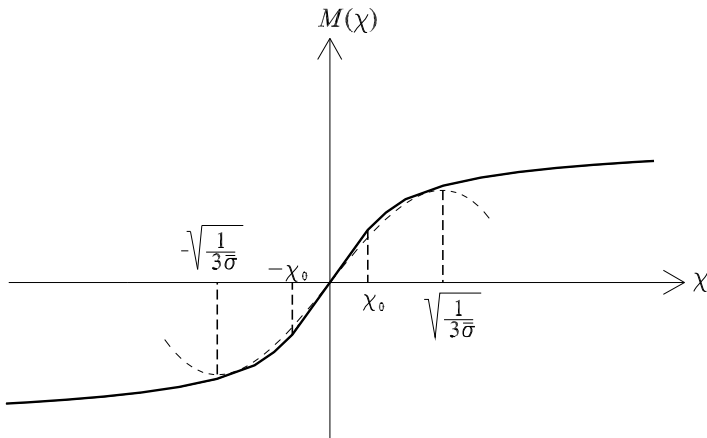


Figure 6. Comparison between equations (3-7) and (4-1).

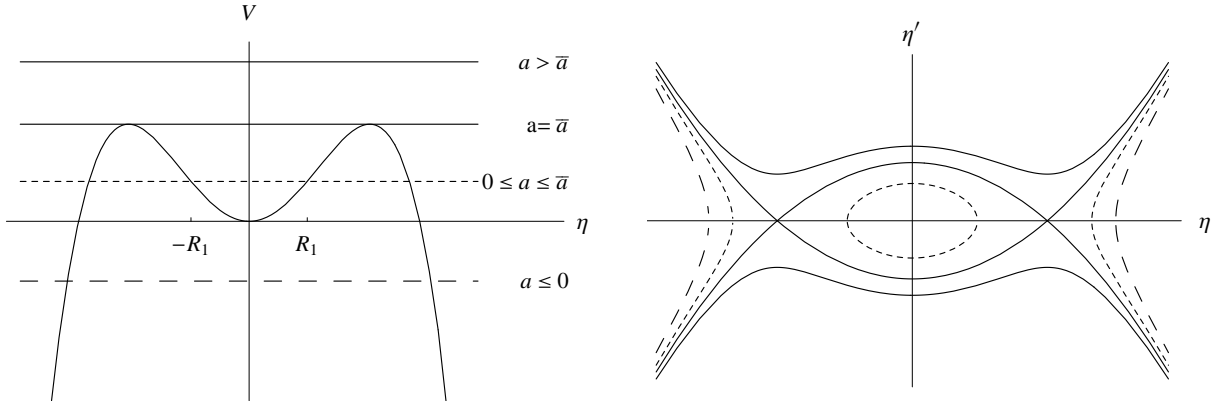


Figure 7. Solutions to the equations of motion for the cubic equation with different values of the total energy a .

Then

$$\omega = 2\pi / \oint \frac{d\eta}{\sqrt{2(a - \frac{1}{2}\pi^4\eta^2 + \frac{3}{8}\sigma\pi^8\eta^4)}} = \frac{\pi}{2} / \int_0^{R_1} \frac{d\eta}{\sqrt{2(a - \frac{1}{2}\pi^4\eta^2 + \frac{3}{8}\sigma\pi^8\eta^4)}}, \quad (4-4)$$

by (2-28), where

$$R_1 = \frac{\sqrt{2}}{\pi^2} \sqrt{\frac{1 - \sqrt{1 - 6a\sigma}}{3\sigma}} \quad (4-5)$$

is the smallest positive root of the equation

$$a - V(\eta) = 0. \quad (4-6)$$

If we draw the graph of the function $V(\eta)$ and represent different values of energy a by horizontal lines (see Figure 7), the condition $a \geq V(\eta)$ can be easily studied in the phase plane $(\eta-\eta')$, observing that, from (2-11), we have

$$\eta' = \sqrt{2(a - V(\eta))}. \quad (4-7)$$

For no-tension materials and under the present hypotheses (neglecting geometric nonlinearities and assuming an infinite material compressive strength), periodic motion is possible for every positive value of a , because V , given by (3-16) and (3-17), is a convex function. In this case, we see that periodic solutions, represented by closed trajectories in Figure 7, are possible only for

$$0 \leq a \leq \bar{a} \quad \text{and} \quad -R_1 \leq \eta \leq R_1. \quad (4-8)$$

From Figure 8, where ω is plotted as a function of a for different values of σ using (4-4), we see that the frequency is a decreasing function of the total energy. All curves originate from the value of the fundamental frequency of the linear beam.

For increasing values of the axial force N , corresponding to decreasing values of σ , the nonlinear behavior becomes weaker.

Let us now consider a hinged-hinged beam subjected to an initial deformation of the form (3-20). With the help of (4-3) and (3-21), we can express the total energy a of the beam as a function of the maximum

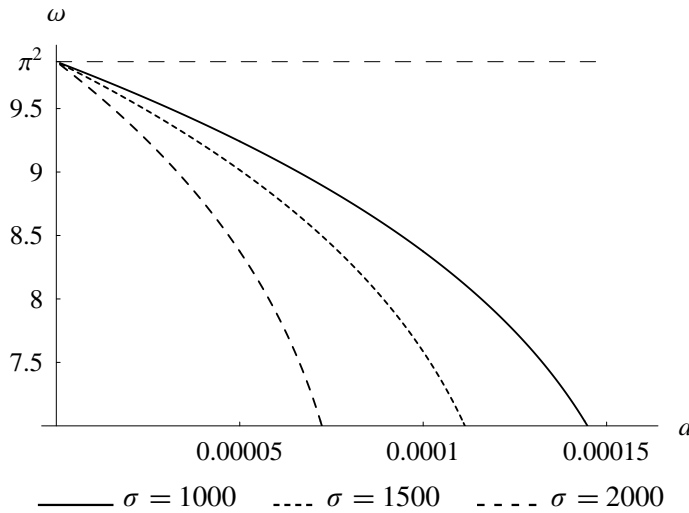
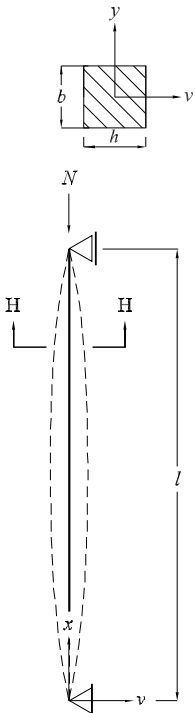


Figure 8. Frequency ω as a function of a for different values of σ .

amplitude A of the motion, $a(A) = V(0) = \frac{1}{4}\pi^4 A^2 - \frac{3}{32}\sigma \pi^8 A^4$. A relation between the fundamental frequency ω and the amplitude A of the motion along the beam can now be obtained by substituting this equality into (4-4).

5. Example applications



Consider a masonry column, of length l , with a square cross-section, hinged at its supports, as in the figure on the left. Let its dimensions and material properties be $l = 7$ m (beam length), $h = b = 0.6$ m (side of cross section), $\rho = 1800$ kg/m³ (material density), and $E = 3 \cdot 10^9$ Pa (modulus of elasticity). We consider an axial force $N = 10^5$ N applied as shown.

Under the previous hypotheses, we can predict the dynamic characteristics of the beam using the relations (3-18) for no-tension materials and, for curvature values near the elastic limit, relation (4-4) for the cubic constitutive equation.

We choose the following parameter values:

$c = \sqrt{EJ/(\rho bh)} = 223.607$ m ² / s	elastic constant of the beam
$\chi_0 = 2N/(Ebh^2) = 0.0003086$ m ⁻¹	limit elastic curvature
$T = 2l^2/(\pi c) = 0.1395$ s	fundamental elastic period
$\nu = 1/T = 7.17$ Hz	fundamental elastic frequency

Figure 9 shows a plot of the constitutive equation (3-7) together with the corresponding cubic approximation (4-1) for $\bar{\sigma} = 528400$ m². Such a value of $\bar{\sigma}$ is obtained by minimizing the function

$$K(\bar{\sigma}) = \int_0^{\sqrt{1/3\bar{\sigma}}} |M_{nt}(\chi) - M_c(\chi, \bar{\sigma})| d\chi,$$

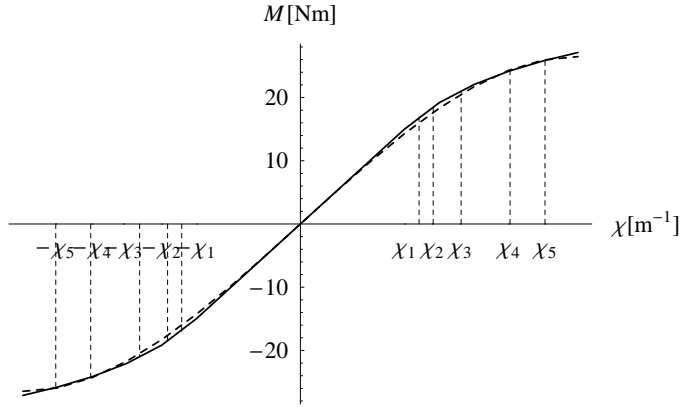


Figure 9. Constitutive equations for the beam section: N.T.M. (solid) and cubic approximation (dashed).

where M_{nt} and M_c are given by (3-7), and (4-1), respectively. We assign the initial displacement

$$v(x, 0) = \bar{A} \sin \frac{\pi x}{l}, \tag{5-1}$$

and consider five cases:

$$\begin{aligned} \bar{A}_1 &= 0.0017 \text{ m} & \chi_1 &= \bar{A}_1 \pi^2 / l^2 = 0.00034 \text{ m}^{-1} \\ \bar{A}_2 &= 0.0019 \text{ m} & \chi_2 &= \bar{A}_2 \pi^2 / l^2 = 0.00038 \text{ m}^{-1} \\ \bar{A}_3 &= 0.0023 \text{ m} & \chi_3 &= \bar{A}_3 \pi^2 / l^2 = 0.00046 \text{ m}^{-1} \\ \bar{A}_4 &= 0.0030 \text{ m} & \chi_4 &= \bar{A}_4 \pi^2 / l^2 = 0.00060 \text{ m}^{-1} \\ \bar{A}_5 &= 0.0035 \text{ m} & \chi_5 &= \bar{A}_5 \pi^2 / l^2 = 0.00070 \text{ m}^{-1} \end{aligned}$$

For beams composed of no-tension materials, the fundamental frequency $\nu_{nt} = \omega / (2\pi T_c)$ is obtained from the relations (3-18) and (3-22), with

$$\kappa_0 = l\chi_0 = 0.0021605, \quad A = \frac{\bar{A}}{l}. \tag{5-2}$$

In this way, we obtain for the fundamental frequencies

$$\begin{aligned} \nu_{1nt} &= 7.166 \text{ Hz} & \nu_{1nt}/\nu &= 0.999 & (\nu_{1c} = 7.042 \text{ Hz} & \nu_{1c}/\nu = 0.982) \\ \nu_{2nt} &= 7.151 \text{ Hz} & \nu_{2nt}/\nu &= 0.998 & (\nu_{2c} = 7.010 \text{ Hz} & \nu_{2c}/\nu = 0.978) \\ \nu_{3nt} &= 7.074 \text{ Hz} & \nu_{3nt}/\nu &= 0.986 & (\nu_{3c} = 6.935 \text{ Hz} & \nu_{3c}/\nu = 0.967) \\ \nu_{4nt} &= 6.849 \text{ Hz} & \nu_{4nt}/\nu &= 0.955 & (\nu_{4c} = 6.766 \text{ Hz} & \nu_{4c}/\nu = 0.944) \\ \nu_{5nt} &= 6.662 \text{ Hz} & \nu_{5nt}/\nu &= 0.929 & (\nu_{5c} = 6.613 \text{ Hz} & \nu_{5c}/\nu = 0.922) \end{aligned}$$

where the corresponding values for the cubic approximation, given by (4-4), are supplied in parentheses.

The results were compared with those obtained by the numerical methods described in [Lucchesi and Pintucchi 2007]. The displacements of the midpoint of the beam have been analyzed via Fourier transform, and the following fundamental frequencies were found:

$$\begin{aligned} \nu_{1num} &= 7.14 \text{ Hz} & \nu_{1num}/\nu &= 0.999 \\ \nu_{2num} &= 7.12 \text{ Hz} & \nu_{2num}/\nu &= 0.993 \\ \nu_{3num} &= 7.02 \text{ Hz} & \nu_{3num}/\nu &= 0.979 \\ \nu_{4num} &= 6.76 \text{ Hz} & \nu_{4num}/\nu &= 0.943 \\ \nu_{5num} &= 6.54 \text{ Hz} & \nu_{5num}/\nu &= 0.912 \end{aligned}$$

Figure 10 (which shows, by way of example, the Fourier transform of the numerical data corresponding to \bar{A}_4) highlights the lower amplitude peaks at the expense of the predominant peak of the fundamental frequency ν_{4num} . Other superharmonic terms are observable near $\nu = 7\nu_4$, the amplitude of which is just 100 times lower than the amplitude of the fundamental. Therefore, the numerical results appear to confirm that the displacements of the beam can be represented by the unimodal expression (3-9), by using the fundamental frequency obtained from (3-18).

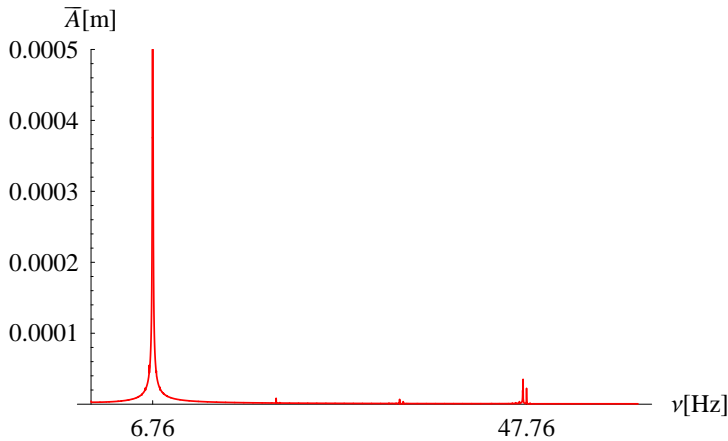


Figure 10. The discrete Fourier transform of the numerical data for $\bar{A} = 0.003m$.

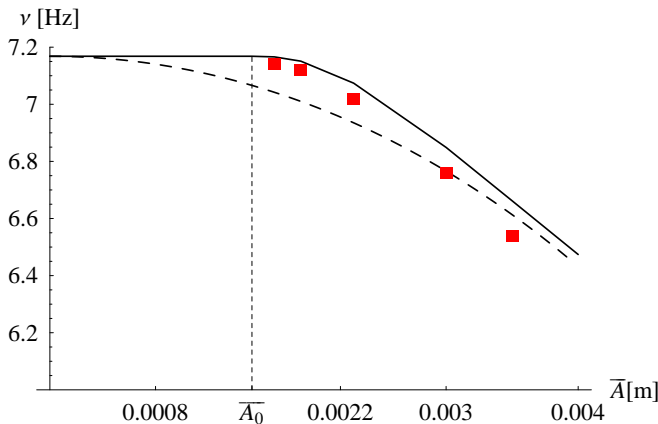


Figure 11. Frequencies obtained via the cubic equation (dashed curve) and the no-tension equation (solid) are compared with the numerical solution (red squares).

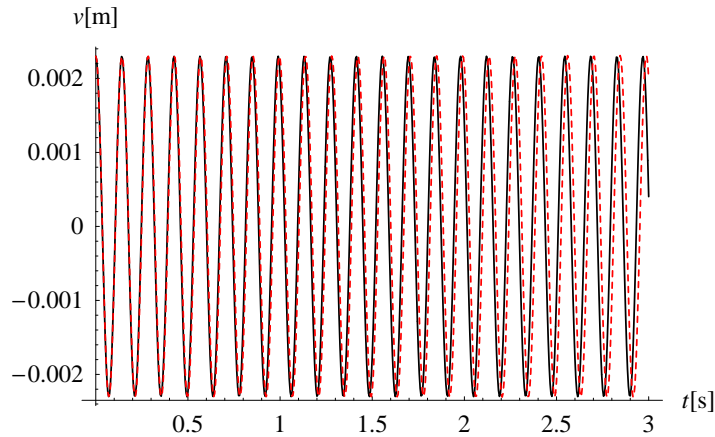


Figure 12. Midpoint displacement of the no-tension material beam for an initial amplitude of $\bar{A}_3 = 0.0023$ m. Solid curve: analytic solution, given by $v(t) = \bar{A}_3 \cos(2\pi \nu_{3nt})$. Dashed curve: numerical calculation. The curves are indistinguishable in the scale of the graph for the first few cycles.

Figure 11 compares the fundamental frequencies obtained using the no-tension equation, the cubic approximation, and the numerical code. The behavior of the cubic equation exhibits more marked softening for small values of \bar{A} due to the absence of the linear elastic region. This difference is reduced for larger values of the amplitude. The numerical results start at values near the no-tension curve and exhibit a more rapid frequency decrease for greater values of \bar{A} .

Lastly, Figure 12 shows the displacement of the midpoint of the beam as a function of time, comparing the explicit solution with the numerical solution.

6. Conclusions

The method presented in this paper yields an explicit relation between the fundamental frequency and the amplitude of the motion for freely vibrating beams composed of nonlinear elastic materials. This method has been applied to slender masonry structures using the constitutive equation for no-tension materials [Zani 2004]. The frequencies, determined analytically for some example applications, are in good agreement with the frequencies predicted from applications of the numerical method presented in [Lucchesi and Pintucchi 2007].

Acknowledgements

We thank Barbara Pintucchi for providing the numerical results presented in Section 5.

References

- [De Falco and Lucchesi 2002] A. De Falco and M. Lucchesi, “Stability of columns with no tension strength and bounded compressive strength and deformability, I: Large eccentricity”, *Int. J. Solids Struct.* **39**:25 (2002), 6191–6210.
- [Del Piero 1989] G. Del Piero, “Constitutive equation and compatibility of the external loads for linear elastic masonry-like materials”, *Meccanica (Milano)* **24**:3 (1989), 150–162.

- [Di Pasquale 1992] S. Di Pasquale, “New trends in the analysis of masonry structures”, *Meccanica (Milano)* **27**:3 (1992), 173–184.
- [Gambarotta and Lagomarsino 1997] L. Gambarotta and S. Lagomarsino, “Damage models for the seismic response of brick masonry shear walls, II: The continuum model and its applications”, *Earthquake Eng. Struct. Dyn.* **26**:4 (1997), 441–462.
- [Girardi 2009] M. Girardi, “Analytical and numerical methods for the dynamic analysis of slender masonry structures”, in *Atti del XIX Congresso dell’Associazione Italiana di Meccanica Teorica ed Applicata* (Paper 103, session ST-09b; full version on accompanying CD), edited by S. Lenci, Aras Edizioni, Ancona, 2009.
- [Girardi and Lucchesi 2006] M. Girardi and M. Lucchesi, “Sulle vibrazioni flessionali di travi costituite da materiale non resistente a trazione”, pp. 135–144 in *WONDERmasonry—Workshop on Design for Rehabilitation of Masonry Structures: tecniche di modellazione e progetto per interventi sul costruito in muratura* (Firenze, 2006), edited by P. Spinelli, Polistampa, Firenze, 2006.
- [Lucchesi and Pintucchi 2007] M. Lucchesi and B. L. Pintucchi, “A numerical model for non-linear dynamic analysis of slender masonry structures”, *Eur. J. Mech. A Solids* **26**:1 (2007), 88–105.
- [Lucchesi et al. 2008] M. Lucchesi, C. Padovani, G. Pasquinelli, and N. Zani, *Masonry constructions: mechanical models and numerical applications*, Lecture Notes in Applied and Computational Mechanics **39**, Springer, Berlin, 2008.
- [MiBAC 2006] Ministero per i Beni e le Attività Culturali, *Linee guida per la valutazione e riduzione del rischio sismico del patrimonio culturale con riferimento alle norme tecniche per le costruzioni*, edited by L. Moro, Gangemi, Roma, 2006.
- [Nayfeh 2000] A. H. Nayfeh, *Nonlinear interactions: analytical, computational, and experimental methods*, Wiley, New York, 2000.
- [Nayfeh and Mook 1995] A. H. Nayfeh and D. T. Mook, *Nonlinear oscillations*, Wiley, New York, 1995.
- [Norme tecniche 2008] Ministero delle Infrastrutture, “Nuove norme tecniche per le costruzioni”, *Gazz. Uff.* **29**:Suppl. Ordinario n. 30 (2008).
- [Petrini et al. 1999] V. Petrini, S. Casolo, and F. Doglioni, “Models for vulnerability analysis of monuments and strengthening criteria”, pp. 179–198 in *Proceedings of the Eleventh European Conference on Earthquake Engineering: invited lectures* (Paris, 1998), edited by P. Bisch et al., Balkema, Rotterdam, 1999.
- [Whitham 1974] G. B. Whitham, *Linear and nonlinear waves*, Wiley, New York, 1974.
- [Zani 2004] N. Zani, “A constitutive equation and a closed-form solution for no-tension beams with limited compressive strength”, *Eur. J. Mech. A Solids* **23**:3 (2004), 467–484.

Received 26 Jun 2009. Revised 1 Oct 2009. Accepted 4 Oct 2009.

MARIA GIRARDI: *Istituto di Scienza e Tecnologie dell’Informazione “A. Faedo”, CNR, Via G. Moruzzi 1, 56124 Pisa, Italy*
Maria.Girardi@isti.cnr.it

MASSIMILIANO LUCCHESI: *Università di Firenze, Dipartimento di Costruzioni, Piazza Brunelleschi 6, 50121 Firenze, Italy*
massimiliano.lucchesi@unifi.it